

Energy-dependent phase-shift analysis of ${}^2\text{H} + {}^4\text{He}$ scattering in the energy range $0.87 < E_d < 5.24$ MeV

V. M. Krasnopol'sky, V. I. Kukulin, and E. V. Kuznetsova
Institute of Nuclear Physics, Moscow State University, 119899 Moscow, U.S.S.R.

J. Horáček

Faculty of Mathematics and Physics, Charles University, V Holešovičkách 2, 18000 Praha 8, Czechoslovakia

N. M. Queen

School of Mathematics and Statistics, University of Birmingham, P.O. Box 363, Birmingham B15 2TT, England

(Received 23 July 1990)

An efficient method for construction of an analytic S matrix from experimental data based on the use of the statistical Padé approximation is proposed. The method is applied to the energy-dependent phase-shift analysis of the elastic scattering of deuterons by alpha particles in the energy range $0.87 < E_d < 5.24$ MeV, and partial-wave phase shifts for $l=0,1,2$ are obtained. In addition, the energies and widths of the three known ${}^6\text{Li}$ resonances are obtained, together with the energy of the ${}^6\text{Li}$ bound state and the vertex constant of the virtual decay ${}^6\text{Li} \rightarrow {}^2\text{H} + {}^4\text{He}$.

I. INTRODUCTION

In a series of papers¹⁻⁵ we have developed a very efficient method for parametrizing experimental data by means of a statistical Padé approximant (also known as a Padé approximant of the third kind or PA-III), i.e., an approximation in the form of a rational function whose coefficients are found by the least-squares method. This technique makes it possible to construct an analytic parametrization of the experimental data which, under certain conditions, provides a stable extrapolation and analytic continuation of various quantities.²⁻⁴ The method has been particularly useful for parametrizing the energy dependence of the S matrix and phase shifts of elastic scattering of light nuclei^{1,2,4} and for parametrizing the angular dependence of the cross sections.^{3,4}

In the present work we apply the technique of statistical Padé approximants to the energy-dependent phase-shift analysis of the elastic scattering of deuterons by ${}^4\text{He}$ in the energy range $0.88 < E_d < 5.24$ MeV. Moreover, we construct an analytic S matrix for this process.

Numerous energy-independent (single-energy) analyses of this system have been carried out,⁶⁻¹⁴ as well as one energy-dependent analysis in the energy range 0.8–1.6 MeV.¹⁵ The purpose of this paper is to report an energy-dependent analysis carried out in a much larger energy range, namely, 0.88–5.24 MeV.

Two methods for phase-shift analysis and parametrization of the data are widely used at present: the R -matrix approach¹⁶ and the S -matrix approach.¹⁰ In the former the function to be parametrized is the R matrix; in the latter it is the scattering function $g_l(p) = p^{2l+1} \cot \delta_l(p)$ (in the simplest case of neutral particles).

Many previous authors¹⁷⁻²⁰ have used the Padé approximation to parametrize the scattering function $g_l(p)$. However, in the majority of cases only the Padé approxi-

mant of the second kind (PA-II) was used.²¹ [We recall that the Padé approximant of the second kind, also known as the N -point Padé approximant, is the rational function which coincides with the function to be approximated at N specified points, whereas the Padé approximant of the first kind (PA-I) is determined by the first N coefficients of the Taylor series of the function at one point. In this sense the PA-II generalizes the Lagrange interpolation polynomials.]

The PA-III has been used by Hartt¹⁸ and Hartt and Yidana¹⁹ for parametrization of model phase shifts calculated with high accuracy.

In this paper we shall apply the PA-III technique to the energy-dependent phase-shift analysis. Moreover, we shall establish the conditions for analytic continuation of the resulting S matrix. Since our technique for calculation of the PA-III differs from other similar approaches,^{18,21,22} we shall describe it briefly in Sec. II. Section III is devoted to the energy-dependent phase-shift analysis of ${}^2\text{H} + {}^4\text{He}$ scattering. This system is extremely useful for our study because it has three sharp resonances in the low-energy region, as well as a weakly bound state, namely, the ground state of ${}^6\text{Li}$, and the determination of the parameters of these states constitutes a stringent test of our approach. The main results of our work are summarized in Sec. IV.

II. CONSTRUCTION OF AN ANALYTIC APPROXIMATION TO THE S MATRIX

There are two ways of constructing an analytic S matrix, which is necessary for an energy-dependent phase-shift analysis. In the first approach all nearby singularities, including the left-hand dynamical cuts, are taken into account explicitly in the ansatz for the S matrix. This *modus operandi* has been widely used by Arndt and

co-workers in their celebrated papers on the energy-dependent analysis of the NV system. Its main advantages are a low number of adjustable parameters and good stability. However, in our case this approach is not useful because the presence of the Coulomb interaction makes the structure of the left-hand dynamical cuts and, in particular, the discontinuities across these cuts very complicated.²³ This is also true of the singularities due to box diagrams. Moreover, because of the angular momentum coupling between subsystems, the number of cuts is large.

Therefore, in what follows we choose a second compromise method. We shall explicitly allow for only the closest and most important cuts and then take advantage of the high flexibility of the Padé approximants. This approach makes it possible to simulate the contribution from the other cuts (i.e., those not included in our original ansatz) either by an effective pole or by alternating zeros and poles of the Padé approximants (see the examples in Ref. 19). To begin with, we shall briefly discuss the process of construction of an analytic S matrix in the case of one-channel scattering. The interaction between the particles is assumed to be a combination of a Coulomb and a short-range part.

A. Consideration of the threshold singularities

In the case of a short-range local interaction, the S matrix has a kinematic square-root singularity at $E=0$ and is a single-valued analytic function of the variable $p = (2\mu E/\hbar^2)^{1/2}$, where E is the c.m. energy and μ is the reduced mass. The l th partial-wave S matrix can be expressed in terms of the analytic scattering function²⁴

$$g_l(E) = p^{2l+1} \cot \delta_l(p), \quad (1)$$

in the form

$$S_l(p) = \exp[2i\delta_l(p)] = \frac{g_l(E) + ip^{2l+1}}{g_l(E) - ip^{2l+1}}. \quad (2)$$

The poles of the S matrix (2) are equivalent to the zeros of the function

$$\begin{aligned} f_l(p) &= g_l(E) - ip^{2l+1} \\ &= p^{2l+1} \cot \delta_l(p) - ip^{2l+1}. \end{aligned} \quad (3)$$

In the case of the short-range plus Coulomb interaction, the second part dominates in the low-energy scattering of charged particles. In this case the threshold singularity becomes more complicated, the function $g_l(E)$ in Eq. (1) is no longer an analytic function of the energy, and the effective-range theory suggests that the function $g_l(E)$ should be replaced by the function

$$g_l^{(c)}(E) = p^{2l+1} C_l^2 [C_0^2 (\cot \delta_l^{(N)} - i) + 2\eta H(\eta)] / C_0^2, \quad (4)$$

which is now an analytic function of the energy,²⁵ so that the problem reduces to the case discussed above. Here $\delta_l^{(N)}$ is the Coulomb-modified phase shift corresponding to the standard decomposition of the total phase shift $\delta_l = \delta_l^{(N)} + \tau_l$, where τ_l is the pure Coulomb phase shift and

$$\begin{aligned} \eta &= Z_1 Z_2 e^2 \mu / \hbar^2 p, \\ C_0^2 &= 2\pi\eta / (e^{2\pi\eta} - 1), \\ C_l^2 &= C_{l-1}^2 (1 + \eta^2 / l^2), \\ H(\eta) &= \psi(i\eta) + \frac{1}{2i\eta} - \ln[-i\eta \operatorname{sgn}(-Z_1 Z_2)], \\ \psi(i\eta) &= -C - \frac{1}{i\eta} + i\eta \sum_{n=1}^{\infty} [n(n+i\eta)]^{-1}, \end{aligned} \quad (5)$$

where μ is the reduced mass and C is Euler's constant. The S -matrix poles are now equivalent to the zeros of the modified function

$$\begin{aligned} f_l^{(c)}(p) &= C_l^2 p^{2l+1} \cot \delta_l^{(N)} - i C_l^2 p^{2l+1} \\ &= g_l^{(c)}(E) - 2\eta p^{2l+1} C_l^2 H(\eta) / C_0^2. \end{aligned} \quad (6)$$

All the expressions (1)–(6) are valid throughout the p plane; i.e., they are valid on both the physical and unphysical sheets (the sheets differ in the sign of $\operatorname{Im} p$). At positive energies the expression (4) can be simplified:²⁵

$$g_l^{(c)}(E) = p^{2l+1} C_l^2 [\cot \delta_l^{(N)} + 2\eta h(\eta) / C_0^2], \quad (7)$$

where

$$h(\eta) = -C - \ln \eta + \eta^2 \sum_{n=1}^{\infty} [n(n^2 + \eta^2)]^{-1}.$$

B. Padé parametrization of the scattering function

We have seen that the S matrix can be represented in terms of the analytic function $g_l(E)$ in the case of a short-range interaction [or $g_l^{(c)}(E)$ in the short-range plus Coulomb case]. To construct the S matrix, it is therefore sufficient to parametrize the scattering functions $g_l(E)$.

The simplest way of parametrizing an analytic function is to truncate its Taylor-series expansion. The Taylor series of the function $g(E)$ in the variable p^2 coincides in our case with the effective-range expansion

$$g(E) = -\frac{1}{a} + \frac{1}{2} r_0 p^2 - \frac{1}{4} P p^4 + \dots, \quad (8)$$

which is well known in scattering theory. [Instead of simple powers, a system of orthogonal polynomials $T_n(E)$ is sometimes used to generalize the effective-range expansion:

$$g(E) = \sum_n a_n T_n(E) \quad (9)$$

(see, e.g., Ref. 26).] Such an expansion will be meaningful only if $g(E)$ is known *a priori* to be a smooth function of energy, and it is suitable only near the threshold. An analytic S matrix can be obtained by fitting the scattering length a , the effective range r_0 , the shape parameter P , etc., to the experimental data.

In many cases it is not sufficient to know the S matrix only in the near-threshold region (e.g., in extrapolating the results of a phase-shift analysis to an energy region where there are no experimental data, in making an analytic continuation into the complex p plane, in searching

for distant singularities, in solving the inverse scattering problem, etc.). In such cases the expansion (8) is useless because its radius of convergence is limited by the nearest singularity of $g(E)$, which (mainly in the case of scattering of loosely bound composite particles) is often very close to the origin. For example, in the case of the nd S -wave doublet channel, the function $g(E)$ has a pole at an energy near -0.7 MeV.²⁷ A similar situation occurs for many other systems, such as ${}^2\text{H} + {}^3\text{H}$ or ${}^4\text{He} + {}^4\text{He}$, where the low partial-wave phase shifts pass through zero [i.e., $g_l(E)$ has a pole] at very low energies. In atomic physics such a situation arises typically at an energy near 0.2 eV (the Ramsauer effect).

In order to allow for the nearest pole singularities, a modified effective-range expansion has been proposed.^{17,20,28} For example, as long ago as the initial period of development of phase-shift analyses, the representation

$$g_l(E) = -\frac{1}{a} + \frac{1}{2}r_0p^2 + \frac{A}{p^2 - p_0^2} \quad (10)$$

was used²⁸ to analyze pp scattering. A similar ansatz was applied to low-energy nd scattering.^{17,20} The pole term is introduced here because the phase-shift analysis is carried out near the energies where $g_l(E)$ has a pole, i.e., where the phase shift passes through zero. In the case of nd S -wave doublet scattering, the phase shift does not pass through zero, but $g_l(E)$ has a pole at low negative energies, so that the scattering length cannot be inferred reliably without a pole term.²⁰ A more general Padé parametrization

$$S = \prod_{n=1}^3 \left[\frac{k + i\beta_n}{k - i\beta_n} \right] \left[\frac{k + i\alpha_n}{k - i\alpha_n} \right]$$

has been proposed²⁹ as a means of solving the inverse scattering problem in the 1S NN channel. Such a parametrization makes it possible to describe correctly the 1S NN phase shifts over a very wide energy range (including the region where the phase shift changes sign).

Apart from its pole singularities, the function $g_l(E)$ generally has dynamical left-hand cuts associated with two- and many-particle unitarity and with exchange processes in the case of composite-particle scattering. In all these cases the parametrization (10) proves to be inadequate. An attempt to simulate the cut by a single pole was proposed for low-energy S -wave doublet $n + {}^2\text{H}$ scattering.¹⁷ It has been found that the approximation of the one-nucleon-exchange cut by a single left-hand pole leads to a representation of the scattering function $g_l(E)$ ($l=0$) in the form

$$g_0(E) = \frac{a + bp^2}{1 + cp^2}, \quad (11)$$

which is a [1,1] Padé approximant.

A representation of the function $g(E)$ which is much more general than (10) or (11), and which takes into account both pole and left-hand cut singularities, can be obtained using the Padé approximant (PA) technique:^{2,18,19,21}

$$g(E) \sim g^{[N,M]}(E) = \frac{P_N(E)}{Q_M(E)}, \quad (12)$$

where P_N and Q_M are polynomials in E of orders N and M , respectively. Under general conditions the representation (12) (known as an $[N,M]$ Padé approximant) converges with increasing N and M in the entire domain of analyticity of $g(E)$. It converges even in the vicinity of a cut, which is simulated by the PA as a series of poles and zeros.³⁰ Its effectiveness has been demonstrated elsewhere.^{2,18,19,21,22} For example, the effective-range expansion for the Yukawa potential was used¹⁹ to construct the PA representation of the partial-wave S matrix. It was found in that paper that the Yukawa cut of the Jost function lying on the negative imaginary k semiaxis was reproduced by alternating zeros and poles of the PA (12).

Evidently, the Padé representation (12) can be used for effective multiple-pole modeling of the dynamical left-hand cuts (in the E plane) and pole singularities simultaneously.

The formulas obtained by this parametrization have a very simple structure. For example, in case of a short-range potential, the resultant partial-wave S matrix is of the rational form

$$S_l(p) = \frac{P_N(E) + ip^{2l+1}Q_M(E)}{P_N(E) - ip^{2l+1}Q_M(E)},$$

and the problem of finding its stable poles (i.e., energies of bound states, energies and widths of resonances, etc.) reduces to that of solving a very simple polynomial equation:

$$P_N(E) - ip^{2l+1}Q_M(E) = 0. \quad (13)$$

In the case of a short-range plus Coulomb interaction, instead of Eq. (13), one must solve the transcendental equation

$$C_0^2 P_N(E) - 2\eta p^{2l+1} C_l^2 H(\eta) Q_M(E) = 0. \quad (14)$$

The residues at these poles are now easy to calculate. The S -matrix residues C_l carry independent physical information, for they in fact give the vertex constants $g_l(s \rightarrow a+b)$ corresponding to the decay of bound or resonance states to a given channel.^{31,32}

C. Calculation of the PA coefficients and construction of initial approximation

We shall determine the coefficients of the polynomials P_N and Q_M (a total of $N+M+1$ independent parameters) in the parametrization (12) by fitting experimental cross sections and vector and tensor analyzing powers using a nonlinear least-squares procedure in an energy-dependent phase-shift analysis. Such a minimization is a cumbersome problem, and since the form of the χ^2 surface in parameter space is very complicated,³³ it is very important to find a good initial approximation for the coefficients. To find such an approximation, any information can be used, namely, phase shifts obtained elsewhere, tentative results obtained by a low-order PA, spectroscopic information (energies and widths), results of

theoretical calculations, etc. These problems have been discussed in detail in the numerous papers by Arndt and collaborators (see, e.g., Refs. 26, 33, and 34) devoted to the problem of NN phase-shift analysis. We shall therefore discuss here only the problems related to the Padé parametrization of the S matrix. In the illustrative examples presented below and in Ref. 2, we assume that the phase shifts δ_i , obtained from energy-independent phase-shift analyses or from theoretical calculations, are known at certain energies E_i with experimental errors $\bar{\varepsilon}_i$. This means that the values of the function $g(E)$, $g(E_i)=g_i$, and their errors ε_i are known. Our task now is to find an optimal (in the sense of the χ^2 criterion) PA for the function $g(E)$.

Minimization of the functional

$$\chi^2 = \sum_{i=1}^k \left| \frac{1}{\varepsilon_i} \left[\frac{P_N(E_i)}{Q_M(E_i)} - g_i \right] \right|^2 \quad (15)$$

in the standard way, i.e., use of the conditions $\partial^2\chi/\partial a_i=0$, leads to a system of nonlinear equations for the coefficients of P_N and Q_M . Such systems are very difficult to solve directly. To facilitate the solution of the problem, several linearized versions of the problem have been proposed.^{13,18,19,21,22} Here we shall briefly discuss only the very effective procedure described in Ref. 2. Each step of the procedure involves the solution of a linear problem resulting from minimization of the functional

$$\tilde{\chi}_s^2 = \sum_{i=1}^k |[P_N^{(s)}(E_i) - g_i Q_M^{(s)}(E_i)]/\varepsilon_i^{(s)}|^2, \quad (16)$$

where

$$\varepsilon_i^{(s)} = \varepsilon_i Q_M^{(s-1)}(E_i), \quad \varepsilon_1^{(0)} = \varepsilon_i, \quad s=0,1,\dots$$

The zeroth iteration coincides with that presented in Ref. 22. This algorithm, unlike the procedure proposed in Ref. 18, involves a calculation of all the coefficients of the polynomials $P_N^{(s)}$ and $Q_M^{(s)}$ simultaneously, thereby resulting in very rapid convergence, at least in most of the cases we have studied.

Now we shall describe the method of fixing the order $[N,M]$ of the optimal PA. On increasing the order of the PA, we usually obtain a rapid (though not always monotonic) decrease of χ^2 . When the approximated experimental data are known with statistical errors, we restrict ourselves to those values of N and M for which $\chi^2/\nu < 1$ (where ν is the number of degrees of freedom, defined as the difference between the number of fitted experimental points and the number of independent adjustable parameters) because, without any additional criterion, all solutions for which $\chi^2/\nu < 1$ are equally acceptable, and it makes no sense to attempt to reach values of χ^2/ν much less than unity. We stress that a decrease in χ^2 does not necessarily mean an improvement of the approximated function $g(E)$, and some other criteria, preferably of a physical origin, must be employed. For example, Levinson's theorem has been used¹⁹ to discard incorrect solutions in a calculation based on very precise input phase shifts. In our case, however, the input experimen-

tal data are rather inaccurate. Moreover, the results of various experimental groups are not always mutually consistent (they have systematic errors). This results in a deterioration of the analytic properties of the approximated function more serious than the violation of Levinson's theorem.

A well-known problem which arises in this method is that when the order of the PA is increased in order to reduce χ^2 , doublets often appear. A doublet is a zero with an accompanying nearby pole having a small residue. Doublets usually appear on the real axis between the experimental points and give a small contribution to χ^2 . Sometimes, instead of doublets, a pole appears outside but very close to the studied energy range. The appearance of such poles and doublets in a particular PA indicates that its order is too high and that the PA is merely reproducing the noise in the experimental data. Evidently, there exists an optimal order of the PA which is achieved when the value of χ^2 is sufficiently small and no doublets or unphysical poles are present. The lower the accuracy of the experimental data and the degree of their consistency, the lower the order of the optimal PA.

Figure 1 shows as a typical example the ${}^2\text{H}+{}^4\text{He}$ phase shifts in the state 3D_3 for energies in the range $2 \leq E \leq 10$ MeV. The experimental data are not mutually consistent in the energy range 2–4 MeV, and they show a clear tendency to decrease at higher energies. However, the phase shifts at the two highest energies make it possible to construct an approximation which increases at higher energies. The results of fitting these data by the PA (12) of various orders $[N,M]$ are collected in Table I. It was assumed that all the data have the same relative error of 10%. The table shows the values of χ^2/ν and the positions of the zeros and poles of the scattering function $g(E)$. By comparing Fig. 1 with Table I, we conclude that the $[1,0]$ Padé approximant (the effective-range expansion) yields reasonably good results only for $E < 7$ MeV. The $[1,1]$ PA gives significantly better results, with a smaller value of χ^2/ν by more than a factor of 3; how-

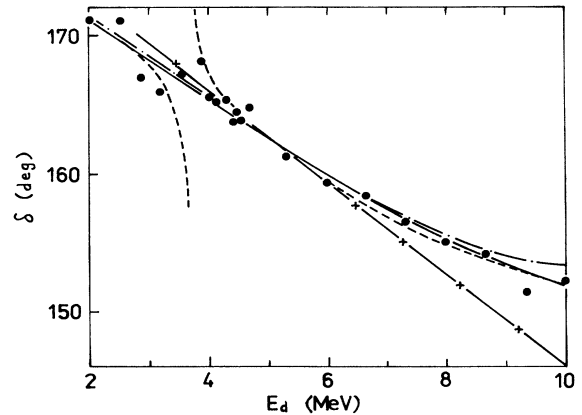


FIG. 1. Approximation of the experimental ${}^2\text{H}+{}^4\text{He}$ phase shift in the 3D_3 state by Padé approximants of the orders $[1,0]$ (dashed line with crosses), $[1,1]$ (dot-dashed curve), $[2,0]$ (solid curve), and $[2,2]$ (dashed curve).

TABLE I. Fits to the data by various Padé approximants.

$[N, M]$	[1,0]	[1,1]	[2,0]	[2,2]
χ^2/ν	5.2	1.5	1.1	2.3
Zeros	1.62	1.26	1.13 -4.6	1.2 3.66
Poles		16.9		3.71 18.5

ever, the high-energy trend of the phase shift is again wrong. This behavior is caused by the penultimate experimental point, which clearly lies outside the general trend. The resulting solution, which is good in the energy range 2–10 MeV, gives phase shifts which increase for $E > 10$ MeV (the scattering function has a false pole at an energy ~ 17 MeV). The [2,0] Padé approximant is the optimal one. It gives the smallest χ^2 value, and its overall behavior is correct. With further increase of the order, the Padé approximant tends to reproduce the noise irregularities of the experimental data. As a result, the [2,2] PA has a doublet (a zero at energy 3.66 MeV and a pole at 3.71 MeV) and a pole at 18.5 MeV. For even higher orders of the PA, the distance between the pole and zero of the doublet becomes smaller, and the solitary pole moves outside the region under investigation. Therefore, to generate an initial approximation for the energy-dependent phase-shift analysis, we recommend the use of an optimal PA satisfying the following two conditions: (1) The value of χ^2/ν is sufficiently small; (2) there are no doublets or false poles in the energy range investigated.

In many cases we also have at our disposal some spectroscopic information such as bound-state energies measured with high accuracy. Such information can be incorporated in our algorithm by slightly modifying the form of the functional (16), while preserving its linearity.² If, for example, the system under consideration has a bound state with energy $E_0 < 0$, the function $f(p)$ [i.e., the denominator of the S matrix (2)] has a zero at $p = p_0 = (2\mu E_0/\hbar^2)^{1/2}$ in the corresponding partial wave. We modify the functional (16) in the following way:

$$\tilde{\chi}_\xi^2 = \tilde{\chi}_s^2 + \xi |f(p_0)|^2, \quad (17)$$

where $\xi |f(p_0)|$ is a penalty function ($\xi \gg 1$ is the penalty coefficient) which leads to a substantial increase of $\tilde{\chi}_\xi^2$ at

$f(p_0) \neq 0$. This modification improves the approximation significantly.

III. ENERGY-DEPENDENT PHASE-SHIFT ANALYSIS OF LOW-ENERGY ${}^2\text{H} + {}^4\text{He}$ SCATTERING

In this section we apply our method to a realistic case which is of great practical importance, namely, the energy-dependent phase-shift analysis of low-energy ${}^2\text{H} + {}^4\text{He}$ scattering. Single-energy analyses of this problem have been carried out previously,^{6–14} and the resonance parameters of ${}^6\text{Li}$ have been obtained. An energy-dependent phase-shift analysis has also been carried out in the low-energy range 0.8–1.6 MeV (Ref. 15); however, because no filtration and selection of the data was used, and the parametrization was rather simple, the results must be treated as preliminary. In particular, the P -wave phase shift obtained in this way is very large and does not agree with the results of other authors. In our approach, using a correct parametrization of the partial-wave amplitudes, we obtain small values of these phase shifts³⁵ in good agreement with other results. Numerous single-energy phase-shift analyses of the ${}^2\text{H} + {}^4\text{He}$ system have already been carried out up to an energy of 13 MeV on the basis of very complete data on differential cross sections, vector and tensor polarizing powers, etc.¹⁴ Unfortunately, such analyses usually do not yield a unique solution, but give several equally acceptable solutions. Moreover, the parameters of resonances obtained in this way depend on the particular parametrization of the partial-wave amplitudes, of the background phase shift, of the energy dependence of the width $\Gamma(E)$, etc. Finally, the main advantage of the energy-dependent phase-shift analyses over the single-energy analysis consists in the fact that for low-energy scattering of spin-1 particles (deuterons), where the data on the vector and especially the tensor analyzing powers are meager and rather imprecise, the energy-dependent phase-shift analysis permits simultaneous use of a much larger amount of data than the single-energy analysis. Also of importance is the correct allowance for the threshold singularities.

A. Parametrization of the low-energy scattering data for ${}^2\text{H} + {}^4\text{He}$ collisions

In the case of low-energy ${}^2\text{H} + {}^4\text{He}$ scattering, the measured cross sections and vector and tensor analyzing powers can be expressed in terms of the partial-wave amplitudes $A_{\nu\nu}$ as⁷

$$\begin{aligned} \frac{d\sigma}{d\Omega} &= \frac{2}{3} \left[|A_{11}|^2 + |A_{10}|^2 + |A_{1-1}|^2 + \frac{1}{2} |A_{00}|^2 + |A_{01}|^2 \right], \\ i\langle T_{11} \rangle &= \left\{ \sqrt{2/3} \text{Im} \left[A_{00} A_{10}^* + A_{01} \left(A_{11}^* - A_{1-1} \right) \right] \right\} / \left[\frac{d\sigma}{d\Omega} \right], \\ \langle T_{20} \rangle &= \left[\frac{d\sigma}{d\Omega} - |A_{00}|^2 - 2|A_{01}|^2 \right] / \left[\sqrt{2} \frac{d\sigma}{d\Omega} \right], \end{aligned} \quad (18)$$

$$\langle T_{21} \rangle = \left\{ -\sqrt{2/3} \text{Re} \left[A_{00} A_{10}^* + A_{01} \left(A_{11}^* - A_{1,-1} \right) \right] \right\} / \left[\frac{d\sigma}{d\Omega} \right],$$

$$\langle T_{22} \rangle = \text{Re} \left[2A_{1,-1} A_{11}^* - |A_{10}|^2 \right] / \left[\sqrt{3} \frac{d\sigma}{d\Omega} \right].$$

The formulas for the scattering amplitudes in terms of the collision matrix $U_{l'l}^J$ are given in Appendix 1 of Ref. 6; the signs of the terms containing off-diagonal S -matrix elements, however, must be reversed.⁷ The S -matrix elements $U_{l'l}^J$ are expressed in terms of the phase shifts ${}^J\delta_l$ and the mixing parameter ε_1 of the 3S and 3D channels as

$$\begin{aligned} U_{00}^1 &= \cos^2 \varepsilon_1 \exp(2i\delta_\alpha) + \sin^2 \varepsilon_1 \exp(2i\delta_\beta), \\ U_{11}^2 &= \exp(2i\delta_1), \\ U_{02}^1 &= U_{20}^1 = \frac{1}{2} \sin(2\varepsilon_1) [\exp(2i\delta_\alpha) - \exp(2i\delta_\beta)], \\ U_{22}^1 &= \sin^2 \varepsilon_1 \exp(2i\delta_\alpha) + \cos^2 \varepsilon_1 \exp(2i\delta_\beta), \\ U_{11}^0 &= \exp(2i\delta_1), \quad U_{22}^2 = \exp(2i\delta_2), \\ U_{11}^1 &= \exp(2i\delta_1), \quad U_{22}^3 = \exp(2i\delta_2). \end{aligned} \quad (19)$$

Here l and l' are the orbital angular momenta of the entrance and exit channels, respectively, J is the total angular momentum, and δ_α and δ_β are the eigenphases, which reduce in the limit $\varepsilon \rightarrow 0$ to the phase shifts ${}^1\delta_0$ and ${}^1\delta_2$ of the states 3S_1 and 3D_1 . It is assumed that $l < 2$ in (19).

An alternative form of energy dependence of the phase shifts can be obtained from Eqs. (7) and (12):

$${}^J\delta_l = \text{arccot} \left[\frac{P_N^{l,J}(E)}{P^{2l+1} Q_M^{l,J}(E)} \frac{1}{C_l^2} - \frac{2\eta h(\eta)}{C_0^2} \right]. \quad (20)$$

The mixing parameter ε_1 can be expressed as

$$\tan \varepsilon_1 = F_N(E) / G_M(E), \quad (21)$$

where F_N and G_M are polynomials in E , and $F_N(0)$ is ap-

proximately equal to the quadrupole moment of the ${}^6\text{Li}$ bound state.

All the parametrizations were obtained by minimizing the functional

$$\chi^2 = \sum_s \sum_i \frac{(N_s X_i^{(s)} - Y_i^{(s)})^2}{\Delta Y_i^{(s)2}}, \quad (22)$$

where $Y_i^{(s)}$ are the experimental values of the cross sections, polarizations, etc., $\Delta Y_i^{(s)}$ are the corresponding experimental errors, $X_i^{(s)}$ are the values of the observables given by the fit, and N_s is a normalization factor for the s th set of data.

B. Data set and construction of the initial approximation

Our analysis is based on a large number of diverse experimental data (cross sections and vector and tensor analyzing powers) obtained by many authors^{6-9,15,36-42} in different energy ranges (see Table II). These data are of variable accuracy, and before the energy-dependent phase-shift analysis is attempted, the data must be made mutually consistent. Consistency is achieved by filtration of the data, which consists of the following selections.⁵

(i) All the subsets for which χ^2/ν is greater than 9 (corresponding to more than three standard deviations) are discarded.

(ii) In the remaining subsets we discard all the points which contribute more than 9 to χ^2/ν , provided that these points are isolated, i.e., that the poor fit to them is not due to a poor fit to the points at neighboring energies.

(iii) In order to allow for different normalizations of the data, we have introduced the normalization coefficients

TABLE II. Description of the data set used in our analysis.

Data set index s	Reference	Data type	Energy range (MeV)	Initial number of data in each set	Final number of data after filtration
1	6	$d\sigma/d\Omega$	0.919–1.228	218	218
2	36	$d\sigma/d\Omega$	0.88–1.6	10	9
3–5	9	$\langle T_{20} \rangle, \langle T_{21} \rangle, \langle T_{22} \rangle$	0.993–1.6	45	45
6	15	$d\sigma/d\Omega$	0.872–1.433	88	88
11	7	$d\sigma/d\Omega$	2.935–4.955	74	57
12	37	$i\langle T_{11} \rangle$	3.0–4.81	30	22
13–15	8	$\langle T_{20} \rangle, \langle T_{21} \rangle, \langle T_{22} \rangle$	2.32–5.24	57	50
21	36	$d\sigma/d\Omega$	1.6–3.51	40	30
22	38	$i\langle T_{11} \rangle$	2.5–4.96	8	8
23–25	39	$\langle T_{20} \rangle, \langle T_{21} \rangle, \langle T_{22} \rangle$	4.25–5.21	12	8
31	40	$d\sigma/d\Omega$	3.4–5.2	53	46
32	41	$i\langle T_{11} \rangle$	2.38–4.95	7	6
33–35	42	$\langle T_{20} \rangle, \langle T_{21} \rangle, \langle T_{22} \rangle$	2.225–5.23	18	5

N_s [see Eq. (22)]. If the value of N_s for a particular group of data is larger than 1.3 or smaller than 0.7, the data group is discarded.

To facilitate the energy-dependent phase-shift analysis, we carried out separate preliminary analyses in two energy ranges, namely, 0.87–1.6 MeV (Ref. 35) and 2.35–5.24 MeV. In the first range we used six data groups $s=1, 2, \dots, 6$ (see Table II), including a total of 361 data points. After filtration of the data as described above, one point was eliminated. The initial approximation was constructed on the basis of the phase shifts given in Ref. 15. The results of the χ^2 minimization in the lower and upper energy ranges are given in Tables III and IV, respectively. Let us consider first the results obtained by using the data in the lower-energy range. Evidently, all the measurements of the differential cross sections in that range ($s=1, 2, 6$) are in good mutual agreement, as the normalization coefficients N_s differ from unity by less than 1%. On the other hand, the data on the analyzing power disagree not only with each other, but also with the cross-section measurements; the coefficients N_s differ from unity by 16–26%. The overall value $\chi^2/\nu=1.36$ indicates that as a whole the data are correctly described. For details of the analysis, see Ref. 35.

In the energy range 2.35–5.24 MeV, we have used 299 points ($s=11-35$; see Table II). Following Ref. 11, we have used a constant normalization coefficient $N_s=0.92$ for the data group with $s=12$ (if this coefficient is allowed to vary and the χ^2 minimization is carried out, we obtain the value $N_s=0.96$).

To determine initial values for the coefficients of the Padé approximants, we have used the phase shifts given in Ref. 11. As a result of the filtration process, the points with $\chi^2/\nu > 9$ were discarded together with the data sets 24, 34, and 35, for which the normalization coefficient differed significantly from unity ($N_{24}=0.1$, $N_{34}=0.44$, and $N_{35}=0.65$). The results based on the remaining data (239 points) are collected in Table IV. The small overall value $\chi^2/\nu=2.1$ indicates a reasonably good description of the data.

The normalization coefficients N_s are also very close to unity for the measurement of the cross sections ($s=11, 21, 31$) and of the vector analyzing powers ($s=12, 22, 32$). For the measurements of tensor analyzing powers, these values differ from unity by 14–25%.

The initial data set for the energy-dependent phase-

shift analysis over the whole energy range 0.87–5.24 MeV was constructed from the two data subsets obtained as described above by filtration of the data within the subranges 0.87–1.6 and 2.35–5.24 MeV and consisted of 592 points.

It is known from a recent single-energy analysis¹⁴ that in this energy range the mixing and absorption parameters are very small and that the phase shifts with $l > 2$ are negligible. Therefore, we restrict ourselves in our energy-dependent phase-shift analysis to real phase shifts for $l=0, 1, 2$ and neglect the mixing of the channels 3S_1 and 3D_1 . Initial values of the coefficients of the Padé approximants were obtained by using the phase shifts in the energy subintervals 0.87–1.6 and 2.35–5.24 MeV, which we obtained in the first stage of our analysis. The phase shifts were approximated by low-order Padé approximants (see Table V), using the linear iterative approach [Eq. (16)]. For a description of the data over the whole energy range, we used Padé approximants with only 19 independent parameters (see Table V); i.e., the number of degrees of freedom was 573.

C. Energy-dependent phase-shift analysis in the range 0.87–5.24 MeV of deuteron energies

The full analysis consists of several steps. First, we set all $N_s=1$ and minimize the χ^2 functional in order to find the values of the Padé parameters. The resulting values of χ^2/ν are summarized in Table VI. The second column contains the results for the initial approximation, and the figures in the third column are the results of the complete minimization. The minimization reduced the value of χ^2/ν from 169 to 3.1. It was also found that all data sets except the one with $s=15$ correspond to values $\chi^2(s)/\nu < 9$. According to the criteria discussed above, we should eliminate this set. However, this is one of the few sets containing the results of measurements of the tensor analyzing power $\langle T_{22} \rangle$, and we have already eliminated one such set ($s=35$, with $\chi^2/\nu=78.1$). We therefore decided to retain this data set in the hope that the in-

TABLE III. Results of the fit in the energy range 0.87–1.6 MeV.

Data set index	N_s	χ^2/ν
s		
1	0.9907	1.4
2	0.9911	2.2
3	0.7640	0.7
4	1.2658	1.5
5	1.1681	1.1
6	1.0059	1.1
Resultant χ^2/ν		1.36

TABLE IV. Results of the fit in the energy range 2.35–5.24 MeV.

Data set index	N_s	χ^2/ν
s		
11	0.9704	2.7
12	0.9974	1.9
13	0.8066	2.0
14	0.8397	2.1
15	0.7485	2.2
21	1.0	2.0
22	0.9661	1.9
23	0.8209	1.3
25	0.8179	0.28
31	1.0034	1.3
32	1.0240	2.5
33	0.8539	0.43
Resultant χ^2/ν		2.1

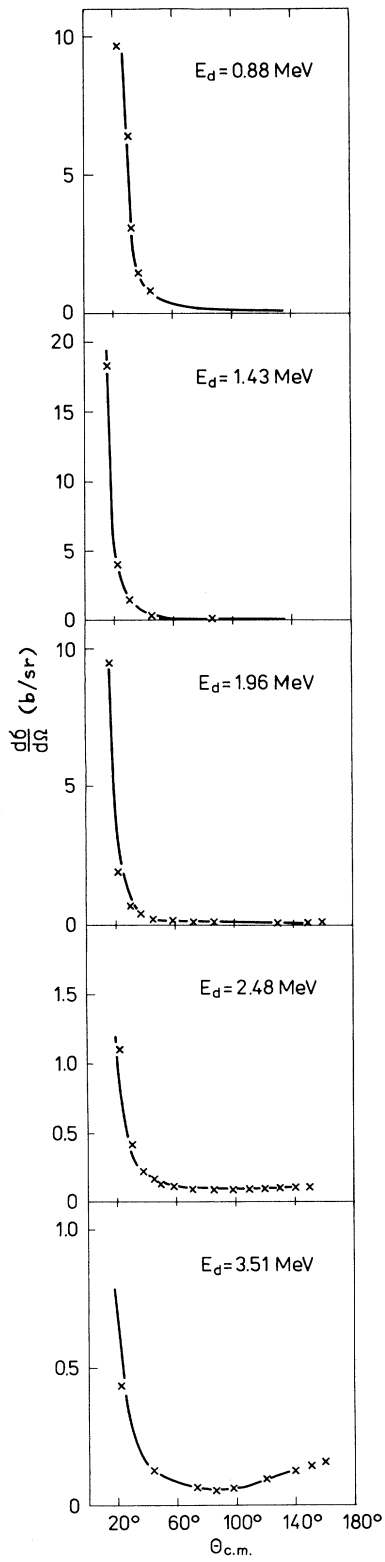


FIG. 2. Differential cross section as a function of the c.m. scattering angle.

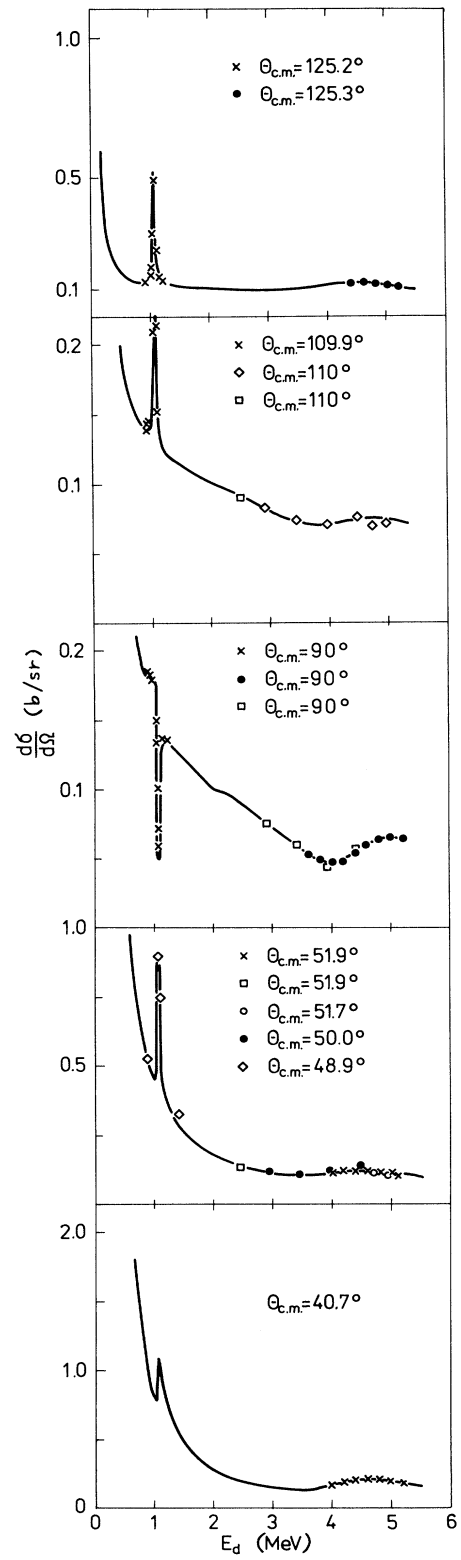


FIG. 3. Differential cross section as a function of the energy.

TABLE V. Orders of the Padé approximants used in the energy-dependent phase-shift analysis in the energy range 0.88–5.24 MeV.

Channel $^{2S+1}L_J$	3S_1	3P_0	3P_1	3P_2	3D_1	3D_2	3D_3
PA order [N, M]	[1,1]	[2,0]	[2,0]	[2,0]	[1,0]	[1,0]	[1,1]
Number of parameters $N_p = N + M + 1$	3	3	3	3	2	2	3

roduction of a variable normalization parameter N_s improves the situation.

In the next stage we allow the normalization coefficients to vary while the Padé coefficients are held constant. The χ^2 values obtained after such minimization are given in the fourth column of Table VI together with the corresponding values of the normalization parameters N_s (fifth column). The value of χ^2/ν for each data set, including the set with $s=15$, is less than 9; i.e., all the sets fulfill our selection criterion. The value of χ^2/ν for $s=15$ is 2.1, but the corresponding normalization coefficient is $N_{15}=0.7363$, which is at the limit of acceptability. The overall value of χ^2/ν was reduced to 2.0 as a result of this procedure.

The large initial value of $\chi^2(s)/\nu$ for $s=31$ indicates that the estimate of the error in these data is probably too low. The situation is less favorable for the data sets $s=21$ and 32, for which the introduction of variable normalization parameters reduces the value of χ^2/ν only

TABLE VI. Results obtained with variable normalization coefficients.

s	Zeroth approx.	Full fit	With variable N_s	
	$\chi^2(s)/\nu$	$\chi^2(s)/\nu$	$\chi^2(s)/\nu$	N_s
1	7.1	1.4	1.4	0.9986
3	2.7	2.1	0.7	0.7623
4	1.6	1.7	1.5	1.2666
5	1.1	1.1	1.1	1.1575
6	0.7	0.9	0.8	1.0126
11	83.9	7.7	2.5	0.9645
12	16.6	5.2	2.6	0.9587
13	16.7	3.4	2.6	0.8545
14	7.4	4.5	1.5	0.8103
15	34.0	10.2	2.1	0.7363
21 ^a	74.0	5.0	4.8	1.0065
22	40.3	6.4	1.5	0.9408
23	5.2	2.7	1.2	0.8423
25	81.1	5.6	0.4	0.8212
31	1916.4	3.4	3.3	1.0011
32	97.6	8.3	7.5	0.9883
33	4.8	1.1	0.7	0.8847
Resultant χ^2/ν	169.5	3.1	2.0	

^aIn the final analysis the data set $s=2$ was combined with the set $s=21$.

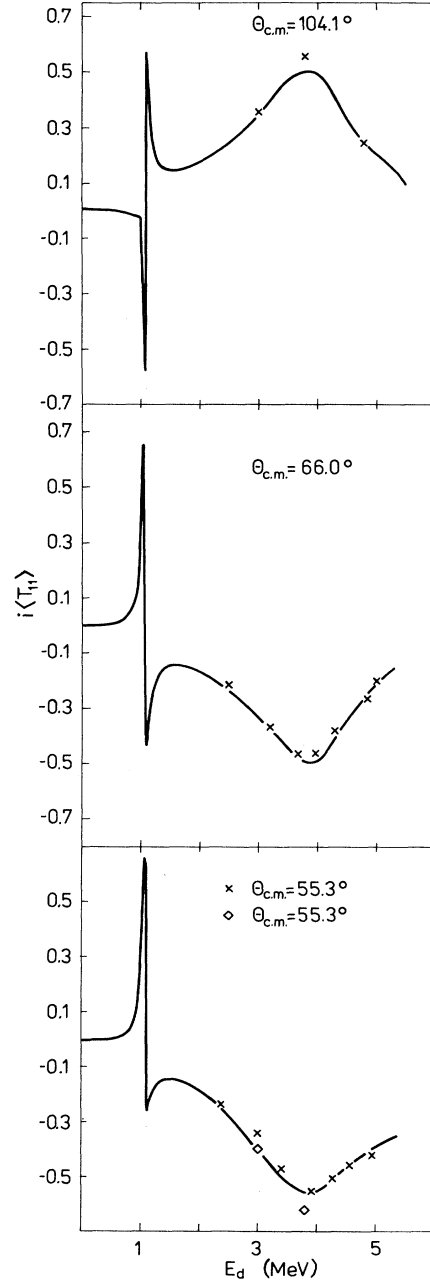


FIG. 4. Analyzing power $\langle T_{11} \rangle$ as a function of the energy.

TABLE VII. Padé parameters^a for the scattering function $g_l^c(E)$ [see Eq. (12)].

$2S+1L_J$	a_0	a_1	a_2	b_1
3S_1	-3.2508×10^{-2}	6.1872×10^{-2}		-4.3373×10^{-2}
3P_0	-1.2783	0.815 08	-0.170 94	
3P_1	-0.192 63	-1.2221	0.227 71	
3P_2	2.0780	-0.903 58	0.135 04	
3D_1	3.1069×10^{-2}	-1.0220×10^{-3}		
3D_2	2.3701×10^{-2}	-4.8650×10^{-3}		
3D_3	5.9730×10^{-3}	-8.0840×10^{-3}		-0.130 53

^aThe parameters are defined by $P_N(E) = \sum_{i=0}^N a_i E^i$, $Q_M(E) = 1 + \sum_{j=1}^M b_j E^j$.

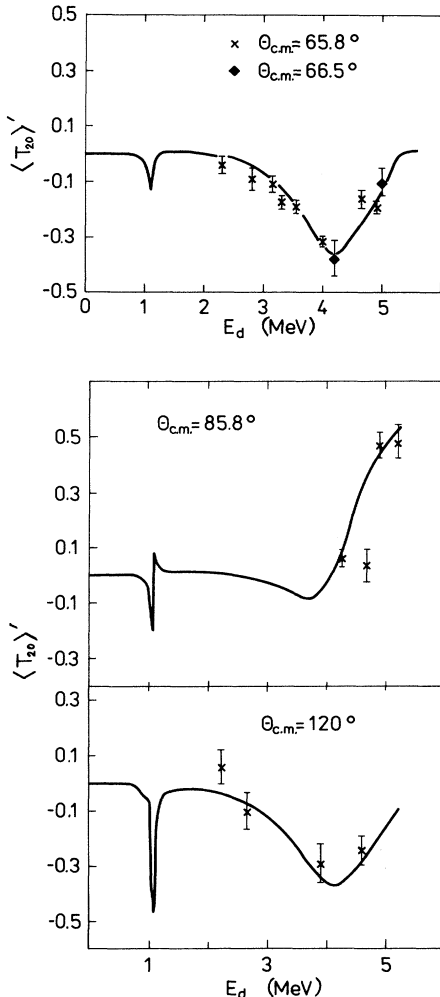
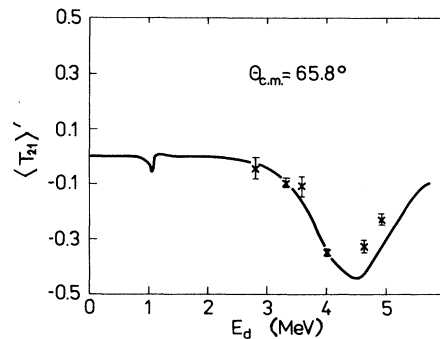
slightly. The data set $s=21$ is an old measurement³¹ of the differential cross section; however, the data in this energy range are very scarce, and we cannot eliminate them completely. The same situation pertains to the data set $s=32$, containing measurements of the vector analyzing power. By comparing the values of N_s for various s , we conclude that (i) the data on the cross sections are in very

good agreement with each other; (ii) the agreement of the polarization data with each other as well as with the cross-section measurements is less satisfactory, and the polarization data are probably subject to a systematic error.

The value $\chi^2/\nu=2$ for our final minimization indicates a very good description of the data. The quality of our fit can be judged also from Figs. 2 and 3, which show the differential cross section as a function of the energy and c.m. scattering angle, and from Figs. 4–7, which show the vector and tensor analyzing powers.

The main results of our analysis, the S and D phase shifts, are displayed in Fig. 8, and the P phase shifts are shown in Fig. 9. The results of single-energy analyses¹¹ are also shown in these figures. We see that our results for the S and D waves are in very good agreement with the results of Schmelzbach *et al.*;¹¹ however, our curve for the P wave is much smoother than theirs, and our phase shifts are also smaller. The dashed curves in Figs. 8 and 9 show the extrapolation of our phase shifts to energies below 0.87 MeV and above 5.24 MeV. Clearly, our analytic S matrix yields a correct extrapolation to distances far from the initial energy range, and this indicates that we have correctly taken into account the basic analytic properties of the S matrix. The values of the Padé coefficients for the modified scattering function $g_l^c(E)$ (giving the phase shifts displayed in Figs. 8 and 9) are given in Table VII.

For all channels except the 3S_1 and 3D_3 channels, a good description of the data is achieved by means of a

FIG. 5. Analyzing power $\langle T_{20} \rangle$ as a function of the energy.FIG. 6. Analyzing power $\langle T_{21} \rangle$ as a function of the energy.

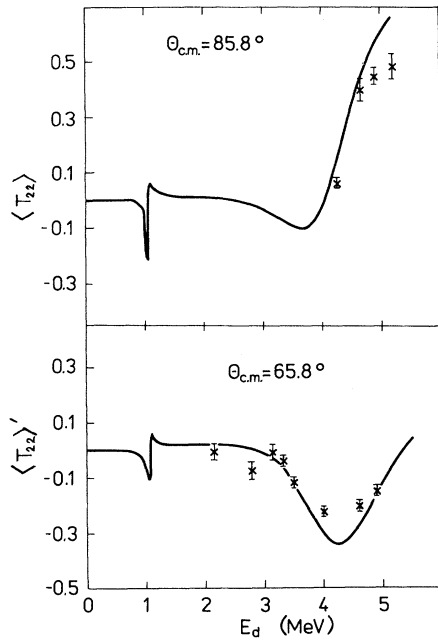


FIG. 7. Analyzing power $\langle T_{22} \rangle$ as a function of the energy.

polynomial approximation of the function $g_f^i(E)$ (see Figs. 8 and 9 and Table VII). For the 3S_1 and 3D_3 channels, a Padé approximant must be used because of the sharp decrease of the 3S_1 phase shift with energy and because of the presence of a narrow resonance in the 3D_3 channel.

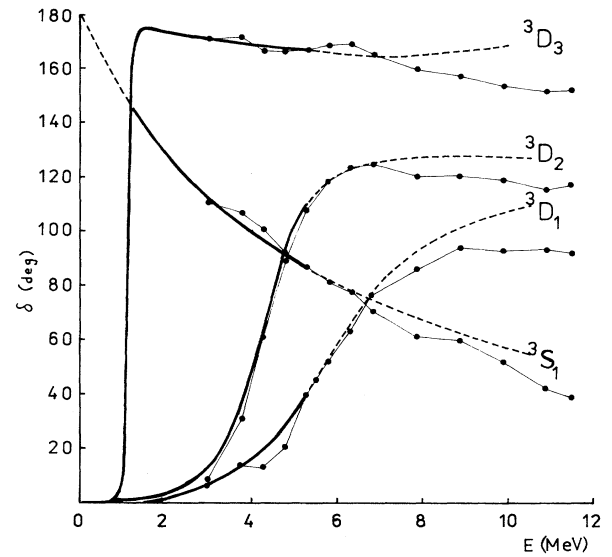


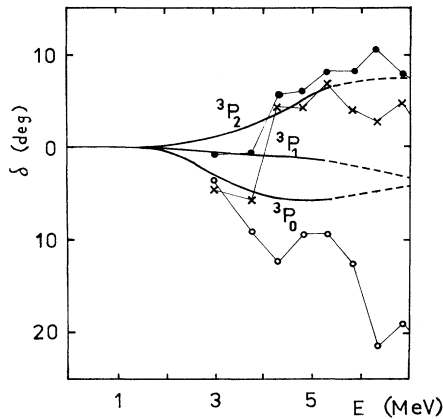
FIG. 8. S and D phase shifts as functions of the energy.

D. Resonance analysis and extraction of low-energy parameters

As we have already noted, our S matrix based on measurements in the energy range 0.87–5.24 MeV describes the phase shifts in a much broader energy range (0–12 MeV); i.e., it makes it possible to carry out a stable extrapolation to the region containing four ${}^6\text{Li}$ states, namely, the ground state in the ${}^3S_1(1^+)$ channel and three reso-

TABLE VIII. Parameters of the ${}^6\text{Li}$ resonance levels with $T=0$ obtained by various authors in chronological order.

L_J	Levels J^π	E_R (c.m.) (MeV)	Γ (c.m.) (MeV)	Reference
D_3	3^+	0.709		7
		0.709		9
		0.715	0.026	10
		0.711 ± 0.002	0.024 ± 0.002	44
		0.713	0.030	present work
D_2	2^+	3.395		7
		3.1		8
		2.81	1.34	10
		3.2		11
		2.835 ± 0.022	1.7 ± 0.2	44
		3.07 ± 0.02	1.6 ± 0.02	13
		2.88 ± 0.04	1.32 ± 0.04	14
2.81	1.07	present work		
D_1	1^+	4.765		7
		4.2		8
		3.54	2.7	10
		4.2		11
		4.2		12
		4.175 ± 0.05	1.5 ± 0.2	44
		4.35 ± 0.06	1.75 ± 0.06	13
		3.82 ± 0.1	1.9 ± 0.1	14
3.88	2.62	present work		

FIG. 9. P phase shifts as functions of the energy.

nances in the channels ${}^3D_3(3^+)$, ${}^3D_2(2^+)$, and ${}^3D_1(1^+)$. These states are found by solving Eq. (14) in the complex p plane. Our results for the energies E_R and widths Γ of the resonance states 3^+ , 2^+ , and 1^+ ($E_R = \text{Re}E_p$, $\Gamma = -2 \text{Im}E_p$, where E_p is the complex energy at which the S matrix has a pole) are compared with the results of other calculations in Table VIII.

This table shows that various calculations give practically the same energy of the 3D_3 state; however, the results for the width differ by 20%. This state was also calculated in our previous analysis in the energy range 0.87–1.6 MeV, where we found $E_R = 0.713$ MeV and $\Gamma = 0.022$ MeV. Thus our phase-shift analysis over the larger energy range has given a significantly larger resonance width, with little change in the resonance energy.

The results for the 2^+ and 1^+ states are much more scattered than those for the 3^+ state. Our results compare well with the results of Ref. 10, obtained by means of an S -matrix parametrization.

The parameters of the effective-range expansion, i.e., the scattering length a , effective range r , and shape parameter P , are collected in Table IX. The values of the effective range r are in all four cases at least an order of magnitude larger than the value of the first term $-1/a$ of the effective-range expansion and are comparable with the value of the shape parameter P . Therefore, the use of the shape-independent approximation is unjustified. Of great interest is the value of the residue at the S -matrix pole corresponding to the ground state of ${}^6\text{Li}$. This residue is closely related to the value of the vertex constant of the virtual decay ${}^6\text{Li} \rightarrow {}^4\text{He} + {}^2\text{H}$. Various values of the vertex constant have been published (see, e.g., Ref. 32).

In order to determine this quantity, we again solved the equation $f_{IJ}(p) = 0$ and found that the S matrix has a pole in the 3S_1 channel at an energy $E_0 = 1.38$ MeV. This value compares well with the exact value 1.47 MeV.

TABLE IX. Low-energy parameters of the even partial waves.

L_J	a	r	P
S_1	30.8	1.88	-2.54
D_3	-167.4	-0.23	0.92
D_2	-42.2	-0.15	
D_1	-32.18	-0.032	

After that we determined the value of the residue C_0 , which is related to the vertex constant G as⁴²

$$C_0 = -(i/\pi)(\mu c/\hbar)^2 G^2.$$

We found the value $G = 0.33$, which is 30% larger than the value obtained by the discrepancy-function method.⁴³

IV. CONCLUSIONS

Our main results can be summarized as follows.

(1) The Padé parametrization of the S matrix (a special case of which is the polynomial representation) constitutes a very efficient means for carrying out an energy-dependent phase-shift analysis based on the data on the differential cross sections and analyzing powers.

(2) By allowing for the analytic properties of the S matrix, provided a sufficient amount of experimental data is available, the phase shifts obtained from the data in a certain energy range can be extrapolated to a larger energy range and also analytically continued to the unphysical energy sheet, thus making it possible to find the resonance poles (and residues) of the S matrix.

(3) Our low-energy results, when combined with the recent very accurate results¹⁴ of the single-energy phase-shift analysis in the energy range 6–43 MeV, make it possible to construct a full description of ${}^2\text{H}+{}^4\text{He}$ elastic scattering from the threshold to 43 MeV.

(4) Our P -wave phase shifts are relatively small and behave smoothly at energies below 7 MeV.

(5) Our resonance energies compare well with the results of other calculations and are probably more accurate than the latter. This is especially true for the states $3+0$ and $2+0$, which lie entirely in the energy range in which the experimental data are available, since we use a single analytic S matrix not only for parametrization of the phase shifts, but also for the analytic continuation to the unphysical energy sheet. This means that we have made a direct determination of the S -matrix poles on the unphysical sheet without recourse to the fitting of Breit-Wigner formulas. The use of Breit-Wigner formulas always raises the question of the energy dependence of the width $\Gamma(E)$.

The authors express their gratitude to Professor I. Ya. Barit for critical discussions, to Dr. N. M. Sobolevsky for help with the error analysis, and to L. N. Brovkina for assistance in the numerical calculations.

- ¹V. M. Krasnopol'sky and S. Chlebnikov, in *Theory of Quantum Systems with Strong Interactions*, edited by A. Gorbato (Kalinin State University, Kalinin, 1983), p. 80.
- ²V. M. Krasnopol'sky, V. I. Kukulin, and J. Horáček, Czech. J. Phys. B **35**, 805 (1985).
- ³J. Horáček, J. Bok, V. M. Krasnopol'sky, and V. I. Kukulin, Phys. Lett. B **172**, 1 (1986).
- ⁴V. M. Krasnopol'sky *et al.*, submitted to Czech. J. Phys.
- ⁵V. I. Kukulin, V. M. Krasnopol'sky, and J. Horáček, *Theory of Resonances: Principles and Applications* (Reidel, Dordrecht, 1988).
- ⁶A. Galonsky, R. A. Douglas, W. Haerberli, M. T. McEllistrem, and H. T. Richards, Phys. Rev. **98**, 586 (1955).
- ⁷L. S. Senhouse and T. A. Tombrello, Nucl. Phys. **57**, 624 (1964).
- ⁸L. C. McIntyre and W. Haerberli, Nucl. Phys. **A91**, 369, 382 (1967); P. Darriulat, D. Garreta, A. Tarrats, and J. Arvieux, *ibid.* **A94**, 653 (1967).
- ⁹H. Meiner *et al.*, Helv. Phys. Acta **40**, 483 (1967).
- ¹⁰L. Kraus, I. Linck, and D. Magnac-Valette, Nucl. Phys. **A136**, 301 (1969).
- ¹¹P. A. Schmelzbach, W. Grüebler, V. König, and P. Marmier, Nucl. Phys. **A184**, 193 (1972).
- ¹²R. A. Hardekopf *et al.*, Nucl. Phys. **A287**, 237 (1977).
- ¹³M. Bruno *et al.*, Nuovo Cimento A **68**, 35 (1982).
- ¹⁴B. Jenny, W. Grüebler, V. König, P. A. Schmelzbach, and C. Schweizer, Nucl. Phys. **A397**, 61 (1983).
- ¹⁵I. Ya. Barit, Yu. G. Balashko, L. S. Dul'kova, and V. P. Zavarzina, Yad. Fiz. **29**, 1137 (1979) [Sov. J. Nucl. Phys. **29**, 585 (1979)].
- ¹⁶A. M. Lane and R. G. Thomas, Rev. Mod. Phys. **30**, 257 (1958).
- ¹⁷S. K. Adhikari, Phys. Rev. C **30**, 31 (1984).
- ¹⁸K. Hartt, Phys. Rev. C **22**, 1377 (1980); **23**, 2399 (1981); **29**, 695 (1984).
- ¹⁹K. Hartt and P. V. A. Yidana, Phys. Rev. C **31**, 1105 (1985).
- ²⁰G. H. Berthold and H. Zankel, Phys. Rev. C **34**, 1203 (1986).
- ²¹F. Nichitiu, Rev. Roum. Phys. **27**, 15 (1982).
- ²²K. Miller, SIAM J. Appl. Math. **18**, 346 (1970).
- ²³L. D. Blokhintsev, A. M. Mukhamedzhanov, and A. N. Safro-
nov, Fiz. Elem. Chastits At. Yadra **15**, 1296 (1984) [Sov. J. Part. Nucl. **15**, 580 (1984)]; L. D. Blokhintsev *et al.*, in *Proceedings of the Tenth European Symposium on Dynamics of Few-Body Systems* (Balatonfüred, Hungary, 1985), p. 22.
- ²⁴J. R. Taylor, *Scattering Theory: the Quantum Theory of Non-relativistic Collisions* (Wiley, New York, 1972).
- ²⁵H. van Haeringen, *Charged-Particle Interactions: Theory and Formulas* (Coulomb, Leyden, 1985).
- ²⁶R. A. Arndt and L. D. Roper, Nucl. Phys. **A209**, 447 (1973).
- ²⁷See, e.g., the review M. P. Locher and T. Mizutani, Phys. Rep. **46**, 43 (1978), and references therein.
- ²⁸M. Cini, S. Fubini, and A. Stanghellini, Phys. Rev. **114**, 1633 (1959).
- ²⁹M. K. Srivastava, P. K. Banerjee, and D. W. L. Sprung, Phys. Lett. **29B**, 635 (1969); D. W. L. Sprung and M. K. Srivastava, Nucl. Phys. **A139**, 605 (1969); M. K. Srivastava and D. W. L. Sprung, *ibid.* **A149**, 113 (1970).
- ³⁰G. A. Baker and P. Graves-Morris, *Padé Approximants* (Addison-Wesley, London, 1981).
- ³¹S. P. Merkuriev, Acta Phys. Austriaca Suppl. **33**, 65 (1981).
- ³²L. D. Blokhintsev, I. Borbely, and E. I. Dolinsky, Fiz. Elem. Chastits At. Yadra **8**, 1189 (1977) [Sov. J. Part. Nucl. **8**, 485 (1977)].
- ³³R. A. Arndt and M. H. MacGregor, in *Methods in Computational Physics*, edited by B. Alder *et al.* (Academic, New York, 1966), Vol. 6.
- ³⁴R. A. Arndt, R. H. Hackman, and L. D. Roper, Phys. Rev. C **15**, 1021 (1977); R. A. Arndt *et al.*, Phys. Rev. D **28**, 97 (1983).
- ³⁵I. Ya. Barit *et al.*, Report No. INR-0513, Moscow, 1987.
- ³⁶J. M. Blair, G. Freier, E. E. Lampi, and W. Sleator, Jr., Phys. Rev. **75**, 1678 (1949).
- ³⁷W. Grüebler, V. König, P. A. Schmelzbach, and P. Marmier, Nucl. Phys. **A134**, 686 (1969).
- ³⁸A. Trier and W. Haerberli, Phys. Rev. Lett. **18**, 915 (1967).
- ³⁹F. Seiler, S. E. Darden, L. C. McIntyre, and W. G. Weitkamp, Nucl. Phys. **53**, 65 (1964).
- ⁴⁰G. G. Ohlsen and P. G. Young, Nucl. Phys. **52**, 134 (1964).
- ⁴¹P. A. Schmelzbach *et al.*, Nucl. Phys. **A264**, 45 (1976).
- ⁴²P. G. Young, G. G. Ohlsen, and M. Ivanovich, Nucl. Phys. **A90**, 41 (1967).
- ⁴³G. R. Plattner, M. Bornand, and K. Alder, Phys. Lett. **61B**, 21 (1976).
- ⁴⁴F. Ajzenberg-Selove, Nucl. Phys. **A320**, 1 (1979).